Check for updates

CHEMISTRY
A European Journal

A Journal of
ChemPubSoc Europe

Accepted Article

Title: Fluorescent pH Responsive Probes Based on Water Soluble BODIPY, Featuring Long Wavelength Emission.

Authors: Gilles Ulrich, Alexandra Sutter, and Mourad Elhabiri

This manuscript has been accepted after peer review and appears as an Accepted Article online prior to editing, proofing, and formal publication of the final Version of Record (VoR). This work is currently citable by using the Digital Object Identifier (DOI) given below. The VoR will be published online in Early View as soon as possible and may be different to this Accepted Article as a result of editing. Readers should obtain the VoR from the journal website shown below when it is published to ensure accuracy of information. The authors are responsible for the content of this Accepted Article.

To be cited as: *Chem. Eur. J.* 10.1002/chem.201801540

Link to VoR: http://dx.doi.org/10.1002/chem.201801540

Supported by
ACES

WILEY-VCH

10.1002/chem.201801540

FULL PAPER

Fully water soluble red emissive pH responsive fluorescent BODIPY derivatives have been synthesized and optical properties investigated.

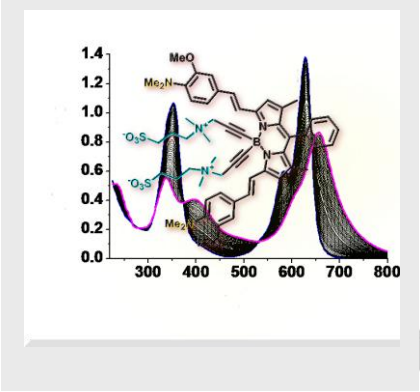

Alexandra Sutter[a] *Mourad Elhabiri,**[b] *and Gilles Ulrich**[a]

Page No. – Page No.
Fluorescent pH Responsive Probes Based on Water Soluble BODIPY, Featuring Long Wavelength Emission.

WILEY-VCH

Accepted Manuscript

This article is protected by copyright. All rights reserved.

10.1002/chem.201801540

WILEY-VCH

Fluorescent pH Responsive Probes Based on Water Soluble BODIPY, Featuring Long Wavelength Emission

Alexandra Sutter[a] Mourad Elhabiri,*[b] and Gilles Ulrich*[a]

Dedication ((optional))

Abstract: We describe here the synthesis of water soluble Red-NIR emissive BODIPY derivatives displaying optical (absorption and emission) responses in pH ranges of interest. Substitution effects close to the tertiary aniline or the phenol subunits selected as the proton sensitive sites allowed us to finely tune the pH ranges. Furthermore, introduction of sulfobetaine functions at the boron centre of these pH responsive BODIPYs afforded valuable fluorescent dyes in the Red-NIR region in aqueous media, for which the steric hindrance and electrostatic repulsions prevent their non emissive aggregation. All the absorption and emission studies, as well as the protonation properties were investigated in aqueous, ethanolic and saline solutions (mimicking physiological conditions). Interestingly, the systems present fluorescent ratiometric protonation response in EtOH but the non protonated form is almost a non fluorescent species under quasi-physiological conditions (saline aqueous solutions) due to the fading of the emissive character of the low lying CT transition in the presence of a supporting electrolyte.

Introduction

The accurate determination of intracellular pH is of critical importance to visualize certain cellular activities or to determine specific pathologies[1] For this purpose, fluorescence microscopy appeared particularly sensitive and has a spatial and temporal resolution over other analytical methods, such as microelectrodes. To reach this goal, it is however necessary to engineer highly luminescent probes that are photochemically and chemically stable under various environmental conditions and highly soluble in water and physiological media. Fluorescent dyes for ratiometric measurements with changes in the fluorescence wavelength are highly desirable for imaging in living cells, due to minimized interference with external factors such as probe concentration, excitation intensity, detector sensitivity, cell size and morphology to cite a few.[2] Moreover, the dyes should be effective preferentially in the biological "open-window" (650-900 nm)[3] to escape from interferences with the biological media and to maximize the sensitivity. These requirements are unfortunately not reached with the current commercial fluorescent dyes for intracellular pH monitoring that suffer from many drawbacks.[1] Most of these fluorescent dyes are indeed based on phenolic class molecule with functions allowing reaching a pK_a around 7-9. The most widely used dyes of this class are based on fluorescein skeleton such as BCECF (2,7,-Bis-(2-CarboxyEthyl)-5-CarboxyFluorescein)[4] or SNARF[5] (SemiNAphtoRhodaFluor). Unfortunately, BCECF is not suitable for ratiometric emission studies (*i.e.,* smart approach to reach precise pH determinations by fluorescence), and SNARF-1 displays a low quantum yield. In addition, intracellular pH measurement cannot be measured accurately under pH 7 due to high pK_a and the optical properties are meaningfully modified by temperature and cell environment.[1,6] An alternative and basic system is HPTS (8-HydroxyPyrene-1,3,6-TriSulfonic acid), a cheap and highly-water soluble dye, but that, however, suffers from high membrane impermeability.[1] Recently, new systems have emerged such as fluorescent rhodamine derivatives[7] or phenol based push-pull systems which have shown ratiometric emissive responses between 500-650 nm and a tuneable range of pK_a by simple substituent variation.[8] A very elegant ratiometric emissive switching system between a fluorescein type-emission in its deprotonated form and an *o*-hydroxybenzazole state with an emission resulting from the enol form of this ESIPT (*i.e.,* Excited State Intramolecular Proton Transfer) emissive system, was described recently and allowed visualizing lysosomal pH changes.[9] Another alternative strategy is to conjugate a tertiary amine to a dye π-system, the protonation of the mesomeric donor group impeding the lone-pair delocalisation and reducing the internal dipole moment. Based on such system, the PYMPON dye, has shown efficient ratiometric pH response in the 3-8 pH range, but the emissions are below 600 nm, and then not suitable for monitoring in blood.[10]. The use of a benzimidazole-based dye system has also recently demonstrated an efficient fluorescent ratiometric response for pH determination in live cell, but the emissions still remain below 600 nm.[11] Dyes from the BODIPY[12,13] family possess interesting features to afford efficient fluorescent pH indicators when adequately functionalized, and many systems[14] were built mostly by conjugation with a tertiary aromatic amine or a phenol moiety.[15] Some of them have been designed to fluoresce in the Red-Near IR region[16] by the way of extended π-delocalization or by use of aza-BODIPY derivatives.[17] These systems are mainly based on fluorescence restoration after protonation of a tertiary amine that is involved in a photon induced electron transfer (PET) or

[a] Alexandra Sutter
Dr Gilles Ulrich
COMBO, ICPEES-UMR 7515
CNRS-Université de Strasbourg
25 rue Becquerel, 67087 Strasbourg Cedex 02, France
E-mail: gulrich@unistra.fr
[b] Dr Mourad Elhabiri
Laboratoire de Chimie Bioorganique et Médicinale, LIMA, UMR 7042
CNRS- Université de Strasbourg
25 rue Becquerel, 67087 Strasbourg Cedex 02, France
E-mail: elhabiri@unistra.fr

Supporting information for this article is given via a link at the end of the document.((Please delete this text if not appropriate))

Accepted Manuscript

This article is protected by copyright. All rights reserved.

responsible of non emissive CT-state. Smart and efficient cancer cells visualization was obtain by use of such pH-activable fluorescence probes in the green region.[18] The same strategy was applied to π-extended systems to reach red region.[19]
In this work, we described the preparation and the spectroscopic properties of water-soluble and highly fluorescent probes in the Red-NIR region that were developed by the introduction of specific function allowing a modulation of the emission wavelength by action of a specific stimulus. The water solubilization techniques recently developed by some of us and adapted to various BODIPY fluorophore thanks to the introduction of Sulfobetaine groups[20] on the central boron atom allowed obtaining highly water soluble and emissive red or NIR emitting BODIPY derivatives.[21] These central zwiterrionic functions prevent aggregation, ensure convenient water-solubility and do not prevent cell penetration.[22] Combining these methodologies, we anticipated to produce water-soluble fluorescent (or ratiometric) pH indicators, based on highly delocalized BODIPY dyes with a tertiary amine donor function having the electron pair implied in the delocalization. The perturbation (or inhibition) of this mesomeric donor property by protons was expecting to modify the emission wavelength, leading to a pH probe. With an adequate choice of substituents with predefined pK_a values, we were able to build fluorescent systems covering different pH ranges. Moreover, this family of BODIPY dyes was shown to have very efficient two-photon cross section[23] that opens up the way to TPA-dyes for visualization of intracellular pH. A thorough spectroscopic and physico-chemical approach has been applied for the characterization of the various protonated species of the pH-sensitive fluorescent dyes based on the BODIPY scaffold examined in this work. Special attention has been paid on the accurate determination of the pK_a values thanks to absorption or emission titrations as a function of pH.

Results and Discussion

Design and synthesis of the BODIPY-based fluorescent systems

To prepare BODIPY dyes emitting in the red-NIR wavelength range, we opted for the use of 3,5-distyryl derivatives, which have been previously shown to display excellent properties in organic solvent as well as in water[16] when properly substituted. Furthermore, such molecular architecture has been shown to be suitable for logic gate[24] applications or acidic gas detection.[25] In addition, we have already developed ratiometric pH sensors in the red-NIR region based on 3,5-distyryl–BODIPY bearing tertiary amine or phenol groups, and demonstrated their brightness and sensitivity in organic solvent or grafted on polymer beads.[26] The synthesis is based on a Knoevenagel condensation between a 3,5-dimethyl-BODIPY and selected benzaldehyde derivatives in the presence of excess of piperidine.[27] To extend this work to water soluble 3,5-distyryl–BODIPY suitable for visualization of pH in biological media, we, however, needed to target several dyes bearing aromatic amines or phenol with different and predefined pK_a values. To reach this goal, specific benzaldehydes have to be synthesized. An aromatic nucleophilic substitution of the fluorine of the commercially available 4-fluoro-3-methoxy-benzaldehyde by a secondary amine (*e.g.,* dimethyl or diethylamine) afforded compounds **1a-b** in good yields (Scheme 1).[28] Based on a previous work,[15] we introduced chlorine at the *ortho* position to the phenol using NCS to lower the pK_a of the phenol unit.[29] Indeed, the protonation constant of a simple phenol (pK_a = 9.80 in water, 0.1 M $NaClO_4$)[30] is decreased by more than 1.5 orders of magnitude upon introduction a chloro function on one of the *ortho* positions (pK_a = 8.25 in water, 0.1 M $NaClO_4$).[30]

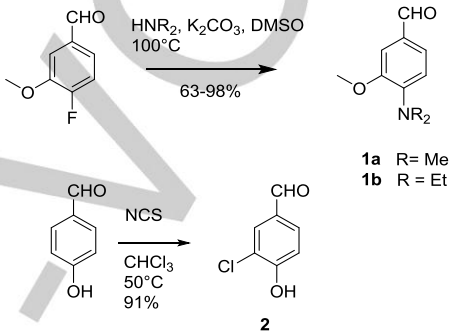

Scheme 1. Synthesis of the substituted benzaldehydes.

The π-extended BODIPY building blocks were then synthesized using a Knoevenagel reaction in the presence of piperidine in toluene with water removal using a Dean-Stark glassware.[26] Using this strategy, mono-styryl BODIPY were obtained using 1 equivalent of benzaldehyde and limited reaction times to afford **3** and **4a** in average yields of 20% (Scheme 2). As a matter of fact, the introduction of a strong electron donating group on 3-position of the boradiazaindacene core facilitate the reaction of the second methyl in 5-position with the carboxaldehyde, leading to increasing amount of 3,5-distyryle compounds (Scheme 2). An important amount of **4e** was isolated from the synthesis of **3**, but can indeed be synthesized in larger amount by reaction of a slight excess of benzaldehyde. Interestingly, during the condensation of 4-hydroxybenzaldehyde on the mono-styryl derivative **3**, in the standard piperidine/toluene (*i.e.,* with a catalytic amount of *p*-TsOH) protocol, the heterodistyryl derivative **4b** (Scheme 2) was obtained in good yields (88%). For the synthesis of **4d** (Scheme 2), the use of 2.5 equivalent of benzaldehyde **1a** in the Knoevenagel condensation procedure led to a high yield of the distyryl derivative (94%). In the case of benzaldehyde **1b** (Scheme 1), the same procedure was applied but significant degradation occurred, and **4c** (Scheme 2) was obtained only in moderate yields (34%).

Accepted Manuscript

This article is protected by copyright. All rights reserved.

10.1002/chem.201801540

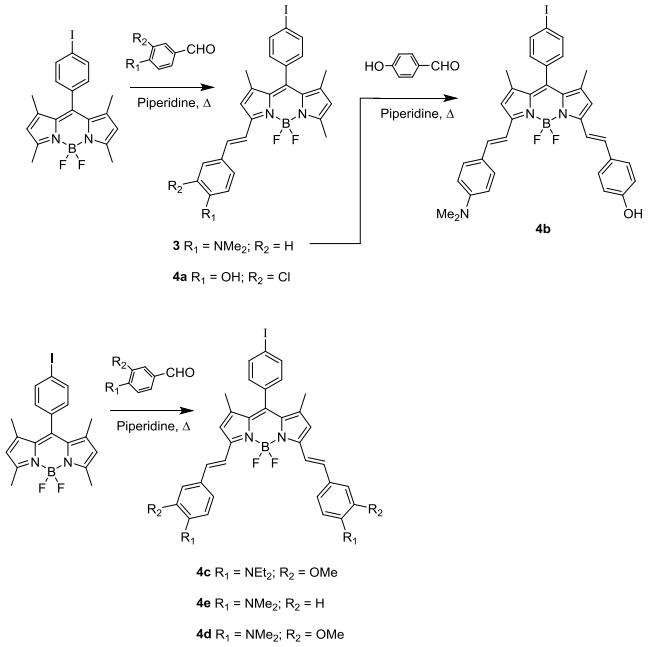

Scheme 2. Synthesis of styryl-BODIPY derivatives.

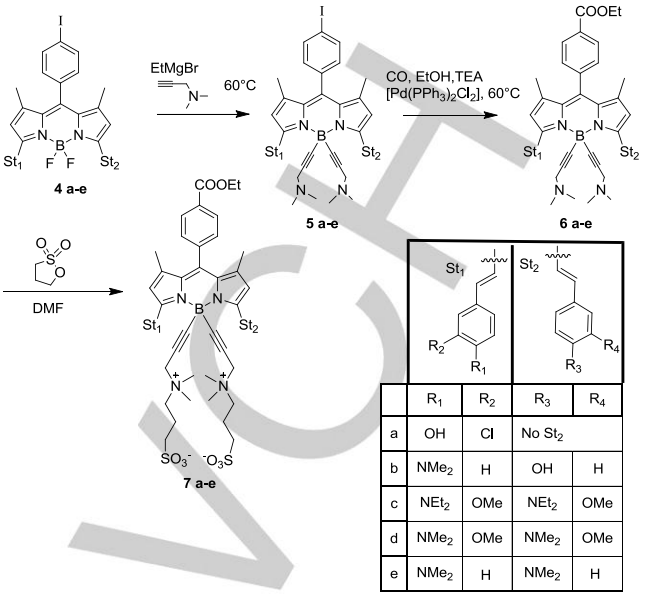

	R1	R2	R3	R4
a	OH	Cl	No St2	
b	NMe_2	H	OH	H
c	NEt_2	OMe	NEt_2	OMe
d	NMe_2	OMe	NMe_2	OMe
e	NMe_2	H	NMe_2	H

Scheme 3. Derivatisation of styryl BODIPY for water solubilization.

To obtain a final probe soluble in water, we then apply the strategy previously developed by some us, which consists firstly of introducing two dimethylamino propyne groups on the boron centres, via the use of the corresponding Grignard derivative.[20,31] Compounds **5a-e** (Scheme 3) were prepared in high yields (50-90%) from the addition of a freshly prepared solution of magnesium dimethylaminopropynide bromide in THF to the BODIPY compound (Scheme 3). Finally, the carbonyl group suitable for a potential labelling or additional water solubilization was introduced via a catalytic carbopalladation reaction.[32] By continuous bubbling of carbon monoxide at atmospheric pressure in a solution of **5a-e** in ethanol/triethylamine mixture and $Pd(PPh_3)_2Cl_2$ as the catalyst, the corresponding ethylester **6a-e** derivatives were obtained in high yields (64-98 %). The last step consists of an alkylation with excess of propane sultone in DMF to obtain the *bis*-sulfobetaine derivatives **7a-e** in moderate yields (Scheme 3). All the final compounds are soluble in water (*ca.* 10^{-4}-10^{-3} M) and have been unambiguously characterized by NMR spectroscopy and elemental analysis.

Optical Properties of the BODIPY dyes

The optical properties of compounds **6-7a-e** were then investigated in dichloromethane (see ESI), EtOH and water (Figure 1 and Table 1). All described derivatives display absorption spectra that are characteristics of BODIPY with styryl pendant arms on the 3 or 3,5-positions,[24-27] with typical high transitions in the orange-red region attributed to the S_0-S_1 transition (Table 1). As previously described for closely related systems displaying a strong electron-donor group on the styryl subunit, the absorption and the emission spectra are sensitive to the solvent dielectric constant. Protonation of either the dialkylamino or the phenolate ionizable sites for the **6a-e** and **7a-e** compounds series systematically induces a strong hypsochromic shift (30-50 nm) of the S_0-S_1 transitions (Table 1), a narrowing of the absorption band due to inhibition of mesomeric electron pair delocalization and the quasi-vanishing of the ICT absorption bands lying in the 390-420 nm spectral range (Figure 1c). The most significant shifts (~ 80 nm) were measured for compounds **6e**/**7e** displaying a dimethylaniline unit on both side arm of the BODIPY scaffold. Similar blue shifts were measured in solvent of weak dipolar moment (hexane) with analogous compounds.[33] In the case of compounds bearing a phenol function on the 3-position, the deprotonation of the later unit induces a significant bathochromic shift due to strong donating ability of the phenolate unit (Figure 1a). In the case of the mixed phenolate/dimethylamino compounds **6**/**7b**, the fully deprotonated species (+76 nm for **6b** and +82 nm for **7b** in EtOH) are characterized by the strongest bathochromic shift with respect to the fully protonated forms due to the subtle combination of +M donating capacities of the tertiary amine and the phenolate units (Figure 1b). Similar behaviours were also observed after protonation or deprotonation in EtOH or water for compounds **7** which possess sulfobetaine solubilizing groups. Concomitantly to the bathochromic shifts of the $S_0 \rightarrow S_1$

Accepted Manuscript

This article is protected by copyright. All rights reserved.

transitions observed upon deprotonation of the pH sensitive units, systematic hypochromic shifts at the absorption maximum were measured for all of the compounds with enlargement of the peak width due to an enhancement of the oscillator strength. These compounds are characterized by a strong internal charge transfer when compared to the standard BODIPY.

Table 1. Optical spectroscopic data for selected compounds.[a]

			Absorption			Emission				
Cmps	Solvent	State	λ_{max} (nm)	$\varepsilon^{\lambda,max}$ (10^4 $M^{-1}cm^{-1}$)	f[b]	λ_{em} (nm)	Φ_F (%)	τ (ns)	k_r (10^7 s^{-1})	k_{nr} (10^7 s^{-1})
6a	EtOH	N	571	5.64	0.23	586	36	5.19	6.92	12.3
	EtOH	D	618	4.13	0.41	727	1.7	0.36	4.72	27.3
6b	EtOH	N	672	6.25	0.38	723	9.3	1.91	4.87	47.5
	EtOH	P	642	6.65	0.29	664	16	2.45	6.53	34.3
	EtOH	D	708	5.69	0.44	776	1.3	0.37	3.51	267
6c	EtOH	N	669	2.38	0.35	770	1	0.6	1.67	165
	EtOH	P	632	3.29	0.35	643	11	4.36	2.52	20.4
6d	EtOH	N	666	5.59	0.54	770	1.1	0.54	2.04	183
	EtOH	P	631	7.26	0.29	645	11	3.58	3.07	24.9
6e	EtOH	N	709	6.11	0.53	766	3.9	1.73	2.25	55.5
	EtOH	P	627	6.93	0.30	640	8.1	2.64	3.07	34.8
7a	EtOH	N	573	4.60	0.19	590	42	4.91	8.55	11.8
	H_2O	N	567	4.25	0.20	582	28	3.2	8.75	22.5
	EtOH	D	631	3.18	0.33	739	1.5	0.39	3.85	253
	H_2O	D	602	3.18	0.32	714	0.4	0.22	1.82	453
7b	EtOH	N	688	7.71	0.46	750	6.2	1.18	5.25	79.5
	H_2O	N	664	5.78	0.52	800	0.3	0.22	1.36	453
	EtOH	P	644	8.69	0.36	665	18	2.38	7.57	34.5
	H_2O	P	635	7.87	0.35	657	18	2.25	8.00	36.4
	EtOH	D	726	7.10	0.55	797	1.2	0.42	2.86	235
	H_2O	D	698	5.97	0.56	797	0.4	0.23	1.74	433
7c	EtOH	N	682	5.02	0.52	814	0.6	0.34	1.76	292
	H_2O	N	662	4.75	0.37	816	0.1	0.22	0.45	454
	EtOH	P	634	8.19	0.29	646	22	4.32	5.1	18.1
	H_2O	P	628	6.65	0.27	643	24	3.73	6.43	20.4
7d	EtOH	N	677	5.80	0.55	799	0.6	0.32	1.88	311
	H_2O	N	664	5.98	0.46	826	<0.01	-		
	EtOH	P	634	9.29	0.31	646	23	3.46	6.65	22.3
	H_2O	P	627	8.26	0.31	641	31	3.71	8.36	18.6

Accepted Manuscript

This article is protected by copyright. All rights reserved.

7e	EtOH	N	714	7.95	0.49	776	5.8	1.44	4.03	65.4
	H_2O	N	697	4.64	0.46	811	0.2	0.25	0.8	400
	EtOH	P	630	9.76	0.34	642	13	1.70	7.65	51.2
	H_2O	P	624	7.35	0.28	640	11	2.31	4.76	38.5

[a]N stands for neutral, P for fully protonated (after addition of aliquots of H_3PO_4 85%) and D for deprotonated (after addition of aliquots of $NaOH_{aq}$ 0.01 M), ε corrected from dilution. Quantum yields calculated using the following standards: rhodamine 6G in water (Φ_F = 0.78, λ_{exc} = 488 nm), cresyl violet in ethanol (Φ_F = 0.50)[34] and tetramethoxydiisoindolomethene-BF_2 in methanol (Φ_F = 0.51).[35] All Φ_F are corrected for changes in refractive index. k_r and k_{nr} were calculated using the following equations: $k_r = \Phi_F/\tau$, $k_{nr} = (1-\Phi_F)/\tau$ assuming that the excited state is obtained with unit efficiency. The uncertainties on the λ_{max}, $\varepsilon^{\lambda max}$ and Q_F are 1 nm, 5% and 10 %, respectively. [b]The oscillator strength **f** was determined using *PHOTOCHEMCAD* software.[36]

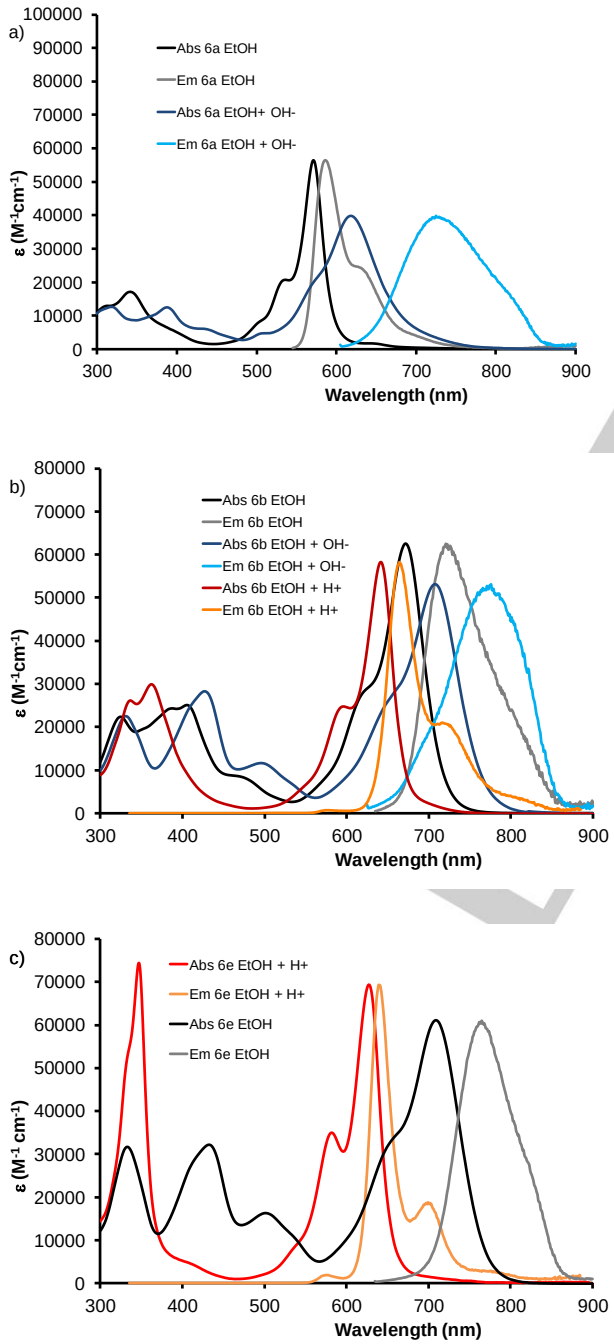

Figure 1. a) Electronic absorption spectra and normalized emission spectra of **6a** under its deprotonated and neutral forms; b) Electronic absorption spectra and normalized emission spectra of **6b** under its protonated, neutral and deprotonated forms; c) Electronic absorption spectra and normalized emission spectra of **6e** under its protonated and neutral forms. Solvent: ethanol; at rt.

The emission spectra are also highly affected by the protonation state of the compounds. For those bearing a phenol group on the styryl side arm (**6a/6b** & **7a/7b**), deprotonation of the phenol unit induces an enhancement of the electron-donating character and led to a strong red-shift of the emission band together with a lowering of quantum yield (Table 1); the increase of the non-radiative rate constant k_{nr} is consistent with an emissive Charge Transfer (CT) state. For compound **6a**, the absorption and emission spectra shifted from an almost classical spectroscopic behaviour of BODIPY to broader and bathochromically shifted spectra after deprotonation (Scheme 1a), with an emission shifting from 586 nm to 727 nm. By contrast, protonation of the tertiary aromatic amine on the styryl arm (**6-7c-e**) arm induces a blue shift of the emission concomitant with a rise of the quantum yields and fluorescence lifetimes (Table 1). The nitrogen being no more available for delocalization, a slight decrease of the non-radiative rate constant is observed as well as a larger radiative rate constant, this phenomenon is in good agreement with a transition from an emissive state with a CT character to a classical S_1-S_0 emission. This is further confirmed by the narrow emissive band and structured vibronic bands, as well as the nearly mirror image of the emission with the S_0-S_1 absorption bands. In the case of the dual compound **6b** and **7b** the emission maximum is shifted from *ca.* 650 nm to *ca.* 800 nm when going from an acidic to a basic environment, with an emission maximum of the neutral state lying at around 720-750 nm in EtOH, as previously observed with *F*-BODIPY systems.[37] As already observed for the absorption studies, the substituents at the boron atom have negligible effects on the optical properties of the dyes, but provide effective water-solubilizing effect and avoid aggregation phenomena. Due to the strong CT character of the emission of the neutral and deprotonated forms, the emission is bathochromically shifted in water (78.4) compared to ethanol (24.5), due to increased dielectric constant, while the emission quantum yield is lowered. Altogether, these optical and electronic properties makes these systems potential interesting ratiometric fluorescent systems in EtOH (and somehow in water). However, it will be shown in the physico-chemical section (*vide supra*) that mimicking biological media with salted aqueous solution (0.1 M) resulted in the complete fading of the emissive character of the low lying CT transition.

Accepted Manuscript

This article is protected by copyright. All rights reserved.

This phenomenon is even more amplified when a supplementary donor group such as a methoxy group is associated to the dialkylamino function on the styryl arm (Figure 2).

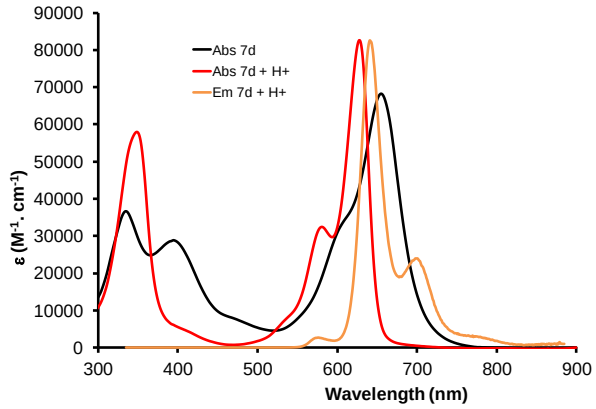

Figure 2. Electronic absorption spectra and normalized emission spectrum of **7d**. Solvent: water; rt.

Acido-basic properties of the BODIPY dyes

To accurately characterize the protonated species of the pH responsive BODIPY probes bearing sulfobetaine solubilizing groups (**7a-e**), we then performed absorption and emission spectrophotometric titrations as a function of pH in water containing 0.1 M NaCl as a supporting electrolyte.

Figure **3** first depicts the absorption and emission spectral variations as a function of pH measured for compound **7a** which bears a phenol pH-sensitive unit. Upon deprotonation of the phenol unit, bathochromic ($\Delta\lambda$ = +32 nm) and hypochromic shifts of the $S_0 \rightarrow S_1$ transitions were observed (Table 3) in agreement with the preliminary optical properties measured in water or EtOH (Table 1). The hypochromic shift of the main absorption is also associated to a significant broadening of this band in agreement with transitions of comparable oscillator strengths (see ESI). The deprotonation of the phenol unit has a marked impact on the emission properties of **7a** as evidenced by the apparent quenching of the $S_1 \rightarrow S_0$ when the pH is increased. The significant decrease of about two orders of magnitude of the absolute quantum yield of **7a** (28% for the neutral species → 0.4% for the deprotonated species, see Table 1) hinders accurate characterization of the deprotonated **7a** species under our experimental conditions. The absorption and emission spectral data sets have been statistically processed and allowed us to properly calculate the protonation constant (pK_a = 6.81(1) and 6.75(3) from absorption and emission titrations, respectively). Importantly, the protonation constant of the *o*-chlorophenolate subunit in **7a** is decreased by about 1.5 orders of magnitude when compared to the reference compound (pK_a = 8.25 for chlorophenol in water at 0.1 M $NaClO_4$)[30] as a consequence of intramolecular conjugation with the BODIPY skeleton. As a consequence, the pK_a value of compound **7a** perfectly matches with the targeted protonation constants suitable for most of the biological applications. Figure 4 gathers the absorption electronic spectra of the protonated species of compound **7a** together with the corresponding distribution diagrams as a function of pH.

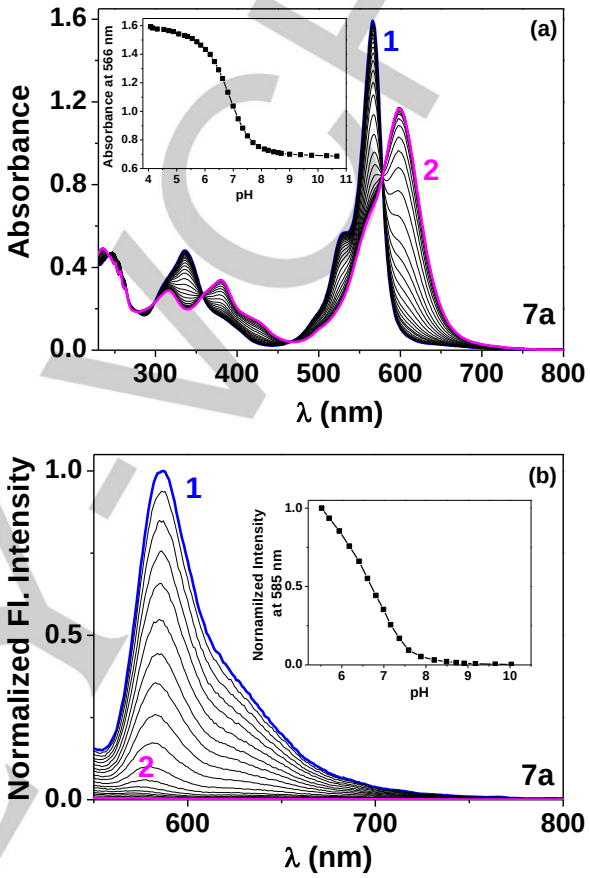

Figure 3. Absorption (a) and emission (b) spectrophotometric titrations of compound **7a** as a function of pH. a) $[\mathbf{7a}]_{tot}$ = 2.0 × 10^{-5} M; (**1**) pH = 4.07; (**2**) pH = 10.67, *l* = 1 cm. b) $[\mathbf{7a}]_{tot}$ = 5.98 × 10^{-6} M; (1) pH = 5.52; (2) pH = 10.03; λ_{exc} = 350 nm; filter = 495 nm; entrance slit = 10 nm; exit slit = 10 nm. Inset: Variation of the emission signal at 585 nm as a function of pH. Solvent: H_2O; *I* = 0.1 M (NaCl); *T* = 25.0(2) °C.

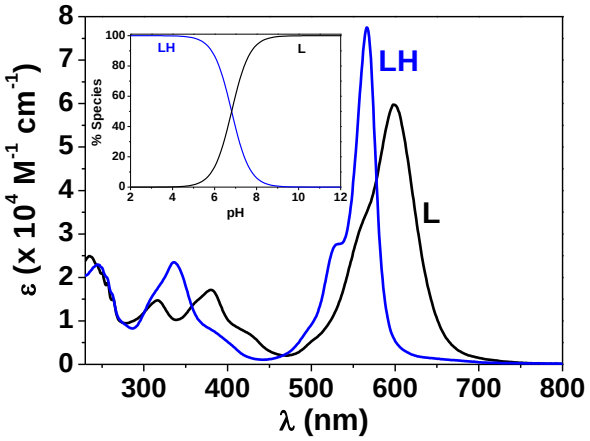

Accepted Manuscript

This article is protected by copyright. All rights reserved.

Figure 4. Electronic spectra of the protonated species of **7a.** Inset: Distribution diagrams of the protonated species of **7a** as a function of pH. Solvent: H_2O; *I* = 0.1 M (NaCl); *T* = 25.0(2) °C. **L** = fully deprotonated species of **7a**. The charges have been omitted for the sake of clarity.

With respect to the aniline based fluorescent probes, we then examined a homogeneous series of compounds (**7c-e**) which only differ by the substitution pattern of the pH responsive unit. Similarly to compound **7a**, we undertook absorption and emission titrations *versus* pH (Figure 5 for **7e** and ESI for **7c-d**) which allowed us to accurately calculate the pK_a values of the ionizable site (Table 2) and to characterize the various protonated species. It is noteworthy that, by contrast with **7a**, compounds **7c-e** are symmetrically substituted on each of the two styryl side arms and are subsequently characterized by two protonation constants. As an example, Figure 5 depicts the electronic spectra of the protonated species of **7e** which contains a *N*,*N*-dimethylamino group on each of the styryl units. The stepwise bathochromic shifts of the $S_0 \rightarrow S_1$ transitions upon deprotonation of the arylammoniums ($\Delta\lambda$ = +41 nm; λ^{max}(**L**H$_2$) = 623 nm and λ^{max}(**L**H) = 664 nm and $\Delta\lambda$ = +59 nm; λ^{max}(**L**H) = 664 nm and λ^{max}(**L**) = 723 nm) as well as the presence of an intense absorption at 348 nm (ε^{348} = 9.45 × 10^4 M^{-1} cm^{-1}) for the diprotonated **L**H$_2$ species are the main features determined for compound **7e** (Table 3). As previously mentioned, the protonation of the *N*,*N*-dimethylamino unit prevent mesomeric electron pair delocalization and thus induces concomitant large stepwise hypsochromic and hyperchromic shifts and sharpening of the $S_0 \rightarrow S_1$ transitions of the BODIPY backbone (*vide supra*). From the absorption versus pH titrations, two close acidic protonation constants have been calculated and were found to be pK_{a1} = 3.10(4) and pK_{a2} = 3.12(5). The second pK_a values has been further confirmed thank to a fluorimetric titration *versus* pH (pK_{a2} = 2.7(1), Figure 5b). The first pK_a value could not be determined under these experimental conditions in agreement with the photophysical data described above (Table 1). These protonation constants are two orders of magnitude lower than the corresponding *N*,*N*-dimethylaniline reference (pK_a = 5.07)[38] as the result of extended mesomeric effects of the monoprotonated **L**H and neutral **L** species. Importantly, it demonstrates that the protonation properties of the luminescent probes can be fine-tuned by a rather simple modification of the terminal ionizable sites and can give rise to potential reporters in a broad range of biological media. As a relevant example, the symmetrical introduction of methoxy group on the *ortho* position of the arylamine (compound **7d**) induces a significant increase of about 2-3 orders of magnitude (pK_{a1} = 4.85(9); pK_{a2} = 5.67(5), Table 3) as a consequence of mesomeric effect of the methoxy to the -N(CH$_3$)$_2$ unit. A stepwise significant increase of the pK_a values toward physiological compatible media (pH ~ 7) is next accomplished by a simple substitution of the arylamine by ethyl substituents (compound **7c**, pK_{a1} = 6.31(5); pK_{a2} = 7.06(3); Table 3). Such effect has been already measured for *N*-alkylated aniline substituted by ethyl substituent (*N*,*N*-dimethylaniline, pK_a = 5.07, *N*,*N*-diethylaniline, pK_a = 6.57). Whatever the compound considered in the **7c-e** series, the luminescence *versus* pH titrations afforded acido-basic properties in good agreement with those evaluated from absorption spectrophotometric studies. In addition, similarly to **7a** bearing a chlorophenol unit, the $S_1 \rightarrow S_0$ transitions of **7c-e** (λ^{em} = 646 nm, 645 nm and 647 nm for the diprotonated states of **7c**, **7d** and **7e**, respectively in water at *I* = 0.1 M NaCl) are apparently quenched upon successive deprotonation (Fig 6b for **7e** and ESI for **7c-d**). This agrees well with the significant drop of the absolute quantum yields of **7c-e** depicted in Table 1 (**7c**: 24% for the protonated species → 0.1% for the neutral species, **7d**: 31% for the protonated species → >0.01% for the neutral species, **7e**: 11% for the protonated species → 0.2% for the neutral species). It was indeed shown that strengthening the electron-donating character of the ionizable sites (*e.g.* by deprotonation) favour the formation of low lying and weakly emissive Charge Transfer (CT) state that is quenched in salted water.

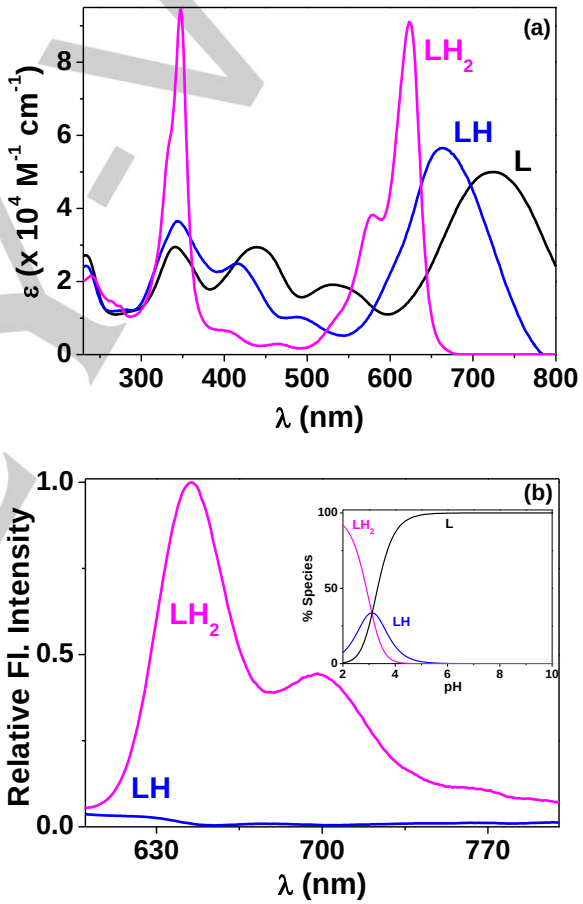

Figure 5. (A) Electronic absorption spectra of the protonated species of **7e.** (B) Normalized Emission spectra of the protonated species of **7e.** Inset: Distribution diagrams of the protonated species of **7e** as a function of pH. Solvent: H_2O; *I* = 0.1 M (NaCl); *T* = 25.0(2) °C. **L** stands for the fully deprotonated species of **7e**. The charges have been omitted for the sake of clarity.

Table 2. Acido-basic properties of compounds **7a-e**.[a]

Accepted Manuscript

This article is protected by copyright. All rights reserved.

Cmpds	log K_1^H (σ)	log K_2^H (σ)
7a	**6.81(1)**[a]**/6.75(3)**[b]	
7b	**8.99(2)**[a]/nd[b]	3.16(5)[a]/3.39(4)[b]
7c	7.06(3)[a]/nd[b]	6.31(5)[a]/6.33(5)[b]
7d	5.67(5)[a]/nd[b]	4.85(9)[a]/5.23(7)[b]
7e	3.12(5)[a]/nd[b]	3.10(4)[a]/2.7(1)[b]

[a]Solvent: water; T = 25.0(2) °C; I = 0.1 M NaCl. [b]from absorption *versus* pH titration. [c]from luminescence *versus* pH titration. nd = not determined. The pK_a values in bold correspond to phenol ionizable sites. Error = σ with σ = standard deviation.

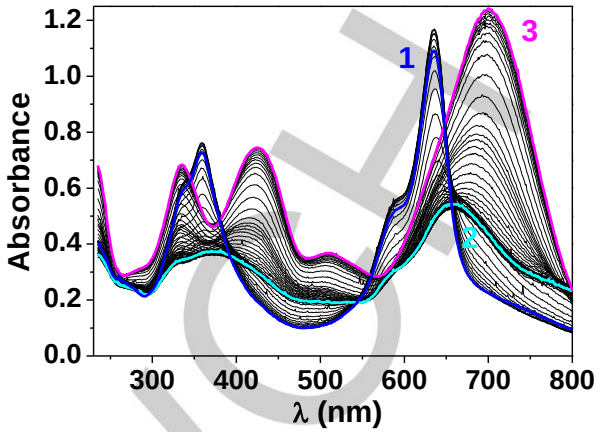

Figure 6. Absorption spectrophotometric titration of compound **7b** as a function of pH. a) $[\mathbf{7b}]_{tot}$ = 1.28 × 10^{-5} M; (**1**) pH = 2.62; (**2**) pH = 4.90; (**3**) pH = 10.62 Solvent: H_2O; I = 0.1 M (NaCl); T = 25.0(2) °C; l = 1 cm.

Figure 6 depicts the absorption spectra *versus* pH of the unsymmetrical distyryl-BODIPY **7b** bearing a phenolate and a *N*,*N*-dimethylaniline protonation. These two ionizable sites have been judiciously chosen for their peculiar protonation properties with respect to the reference compounds discussed above. The statistical processing of the absorption and pHmetric data allowed us to accurately calculate all the pK_a values (Table 1). For **7b**, the two pK_a values (pK_{a1} = 3.16(5) and pK_{a2} = 8.99(2)) agree quite well with reference compounds under identical experimental conditions (phenol: pK_a = 9.91[39] and **7e**: pK_{a1} = 3.12(5)). The diprotonated monocationic species **L**H_2^+ (**L** = **7b**) is characterized by a sharp absorption band centred at 635 nm (ε^{635} = 84 700 M^{-1} cm^{-1}) in the visible region ($S_1 \rightarrow S_0$ transitions characteristics of the BODIPY core). Upon deprotonation of the anilinium subunit, bathochromic (Δλ = +26 nm) and hypochromic shifts are observed together with a large broadening in agreement with the previously discussed features on aniline-based luminescent pH probes (**7e**, Figure 6 and Table 3). Further deprotonation of the phenol moiety led to a further bathochromic shift of the BODIPY-centred transitions (Δλ = +39 nm) as well as a hyperchromic shift. Luminescence titration *versus* pH allowed us to quantify only the protonation properties of the aniline/anilinium pair (pK_{a1} = 3.39(4)). Only the monocationic diprotonated system **L**H_2^+ appears to be a strong emitting unit, deprotonation of the anilinium or the phenol unit resulting to an apparent weak to non emitting species likely due to formation of weakly emissive CT state (*vide supra*).

Table 3. Electronic absorption properties of the protonated species of compounds **7a-e**.[a]

	λ_{max} (nm) [ε (x 10^4 M^{-1} cm^{-1})]		
Cmpds	**L**H_2	**L**H	**L**
7a		317 (sh) 336 (2.35) 529 (2.75) 566 (7.75)	317 (1.47) 380 (1.71) 427 (sh) 598 (5.98)
7b	337 (sh) 359 (1.81) 589 (sh) 635 (8.47)	309 (2.07) 378 (2.28) 661 (3.36)	334 (4.41) 424 (4.81) 506 (2.31) 700 (8.11)
7c	353 (5.16) 584 (2.88) 628 (6.69)	346 (3.46) 424 (sh) 639 (4.85)	337 (2.76) 396 (2.03) 657 (4.37)
7d	351 (6.44) 581 (3.75) 627 (8.91)	343 (4.07) 410 (sh) 596 (sh) 642 (6.50)	335 (3.42) 396 (2.83) 606 (sh) 657 (6.23)
7e	348 (9.45) 579 (3.82) 623 (9.10)	342 (3.65) 416 (2.49) 489 (1.03) 664 (5.65)	341 (2.95) 439 (2.94) 528 (1.91) 723 (5.00)

[a]Solvent: water; T = 25.0(2) °C; I = 0.1 M NaCl. The errors on the λ and ε are estimated to be ±1 nm and 5%, respectively.

Accepted Manuscript

This article is protected by copyright. All rights reserved.

Conclusions

In this study, we were able to synthesize water soluble Red-NIR emissive BODIPY derivatives with meaningful alterations both of their absorption and emission properties in selected ranges of pH. The selection of the pH responsive ranges was obtained by a subtle variation of the substituents close to the tertiary aniline derivatives or the phenol subunits that were chosen as the (de)protonation sites. These units were introduced due to their peculiar electronic properties (i.e., strong mesomeric donors upon deprotonated state). Furthermore, the introduction of sulfobetaine functions at the boron centre of these pH responsive BODIPYs afforded valuable fluorescent dyes in aqueous media, for which the steric hindrance and electrostatic repulsions prevent their non emissive aggregation. The absorption and emission spectrophotometric investigations as well as their pK_a determinations were thus performed both in water (and EtOH) as well as in saline solutions (i.e., mimicking physiological conditions). Most of the investigated systems behave as interesting fluorescent dyes in the Red-NIR region with a high potential for intracellular pH determinations, the pH range of performance being predefined by the substitution pattern close to the protonation sites. However, these systems did not act as efficient fluorescent ratiometric pH probes in quasi-physiological conditions due to the fading of the emissive character of the low lying CT transition in the presence of a supporting electrolyte. We are now investigating analogous systems with weaker CT states in the non protonated forms, which could open the way to the development of fluorescent ratiometric probes in the Red-NIR region for pH measurements.

Experimental Section

Starting Materials, Solvents and general methods

Distilled water was further purified by passing it through a mixed bed of ion-exchanger (Bioblock Scientific R3-83002, M3-83006) and activated carbon (Bioblock Scientific ORC-83005) and was de-oxygenated by CO_2- and O_2-free argon (Sigma Oxiclear cartridge) before use. All the stock solutions were prepared by weighing solid products using an AG 245 Mettler Toledo analytical balance (precision 0.01 mg) and quantitative dissolution in O_2-free water. The ionic strength was maintained at 0.1 M with sodium chloride (NaCl, SDS, Ph. Eur.), and all measurements were carried out at 25.0(2) °C. Standard reagents were purchased from commercial sources and used without further purification. Chromatographic purification was conducted using standard silica gel 60 (0.063-0.200 mm) or deactivated aluminium oxide (Act. III). Thin Layer Chromatography (TLC) was performed on silica gel plates coated with fluorescent indicator. All mixtures of solvents are given in *v/v* ratio. Anhydrous solvents were obtained by distillation: anhydrous CH_2Cl_2 over P_2O_5. ^1H and ^{13}C spectra were recorded at room temperature with 200 MHz, 300 MHz, 400 MHz or 500MHz spectrometers using perdeuterated solvents as internal standards. Chemical shifts of ^1H and ^{13}C spectra are given in ppm relative to residual protiated solvent or relative to the solvent, respectively. UV-visible spectra were recorded using a dual-beam grating spectrophotometer and 1 cm quartz cells. All fluorescence spectra were corrected from 250-850 nm (manufacturer files). The fluorescence quantum yield (Φ_{cmp}) was calculated from equation 1:

$$\Phi_{\mathrm{cmp}} = \Phi_{\mathrm{ref}} \frac{\mathrm{I}}{\mathrm{I}_{\mathrm{ref}}} \frac{OD_{ref}}{OD} \frac{n^2}{n_{ref}^2}$$

Here, *I* denotes the integral of the corrected emission spectrum, *OD* is the optical density at the excitation wavelength and η is the refractive index of the medium. The reference system used were rhodamine 6G (Φ_{em} = 0.78 in H_2O) and cresyl violet (Φ_{em} = 0.53 in CH_3OH).[34] Emission wavelengths were selected by a monochromator. Lifetimes were deconvoluted with adequate software using a light-scattering solution (LUDOX) for the instrument response.

Potentiometric measurements

The potentiometric measurements were performed using an automatic titrator system 794 Basic Titrino (Metrohm) fitted with a combined glass electrode (Metrohm 6.0234.500, Long Life) filled with 0.1 M NaCl in water and connected to a microcomputer (Tiamo light 1.2 program for the acquisition of the potentiometric data). The combined glass electrode was calibrated as a hydrogen concentration probe by titrating known amounts of hydrochloric acid (~10^{-1} M from HCl, Riedel-de-Haën, puriss pa, 37% min) with CO_2-free sodium hydroxide solution (~ 10^{-1} M from NaOH, BdH, AnalaR). The HCl and NaOH solutions were freshly prepared just before use and titrated with sodium tetraborate decahydrate ($B_4Na_2O_7.10H_2O$, Fluka, puriss, p.a.) and potassium hydrogen phthalate ($C_8H_5KO_3$, Fluka, puriss, p.a.), respectively, using methyl orange (RAL) and phenolphthalein (Prolabo, purum) as the indicators. The cell was thermostated at 25.0 ± 0.2 °C by the flow of a Lauda E200 thermostat. A stream of Argon, pre-saturated with water vapour, was passed over the surface of the solution. The Glee program[40] was applied for the glass electrode calibration (standard electrode potential E_0/mV and slope of the electrode/mV pH^{-1}) and to check carbonate levels of the NaOH solutions used (< 5%).

UV-visible absorption titrations *versus* pH

An aliquot of 40 mL of the pH-sensitive dye (**7a**: 2.03 × 10^{-5} M; **7b**: 1.28 × 10^{-5} M; **7c**: 2.06 × 10^{-5} M; **7d**: 2.00 × 10^{-5} M; **7e**: 2.18 × 10^{-5} M) was introduced into a jacketed cell (Metrohm) maintained at 25.0 ± 0.2 °C by the flow of a Lauda E200 thermostat. The free hydrogen ion concentrations were measured with a combined glass electrode (Metrohm 6.0234.500, Long Life) which was calibrated as a hydrogen concentration probe as described above. The initial pH was adjusted to ~ 2-4 with HCl, and the absorption titrations (**7a**: 4.07 < pH < 10.67; **7b**: 2.62 < pH < 10.62; **7c**: 3.02 < pH < 9.27; **7d**: 2.54 < pH < 7.52; **7e**: 2.81 < pH < 10.40) were then carried out by addition of volumes of NaOH solutions (BdH, AnalaR). After each addition (*i.e.* the volume and thereby the pH increments along the absorption *versus* pH titrations were automatically adjusted by the potentiometric system according the signal variation of the solution; the DET (dynamic Potential Titration) method of the Tiamo program was used with a measuring point density of 3), an absorption spectra was repeatedly recorded using a Varian CARY 50 spectrophotometer fitted with Hellma optical fibres (Hellma, 041.002-UV) and an immersion probe made of quartz suprasil (Hellma, 661.500-QX) and interfaced (Cetrib) with the potentiometric unit.

Luminescence Titrations *versus* pH

An aliquot of 40 mL of the pH-sensitive dye (**7a**: 5.98 × 10^{-6} M; **7b**: 5.75 × 10^{-6} M; **7c**: 5.59 × 10^{-6} M; **7d**: 5.98 × 10^{-6} M; **7e**: 6.20 × 10^{-6} M) was introduced into a jacketed cell (Metrohm) at RT. The initial pH was adjusted to acidic values (pH 2-5) with HCl, and the luminescence titrations (**7a**: 5.52 < pH < 10.03; **7b**: 3.39 < pH < 10.94; **7c**: 3.30 < pH < 9.37; **7d**: 3.42 < pH < 9.59; **7e**: 2.29 < pH < 6.18) were carried out by

Accepted Manuscript

This article is protected by copyright. All rights reserved.

addition of known volumes of NaOH solutions BdH, AnalaR) with an Eppendorf microburette. The luminescence emission spectra (550-800 nm) were recorded on a Horiba Jobin Yvon spectrofluorimeter (Fluoromax 4) equipped with optical fibres and immersion probe. The excitation wavelength was selected in the UV region and corresponded to either isosbestic point or the smallest absorbance amplitudes measured along the absorption spectrophotometric titrations. Besides, spectrofluorimetric variations of the $S_1 \rightarrow S_0$ BODIPY transitions were monitored at absorbances < 0.1 to minimize reabsorption processes. The following parameters were used for compounds **7a-e**: **7a**: λ_{exc} = 350 nm; entrance and exit slits = 10 nm; filter = 495 nm; **7b**: λ_{exc} = 363 nm; entrance slit = 14 nm and exit slit = 20 nm; filter = 550 nm; **7c**: λ_{exc} = 360 nm; entrance and exit slits = 20 nm; filter = 550 nm; **7d**: λ_{exc} = 360 nm; entrance slit = 20 nm and exit slit = 12 nm; filter = 550 nm; **7e**: λ_{exc} = 363 nm; entrance slit = 10 nm and exit slit = 20 nm; filter = 550 nm.

Analysis and Processing of the Spectroscopic Data.

The spectrophotometric data were analyzed with Specfit[41-43]program which adjusts the absorptivities and the stability constants of the species formed at equilibrium. Specfit uses factor analysis to reduce the absorbance matrix and to extract the eigenvalues prior to the multiwavelength fit of the reduced data set according to the Marquardt algorithm.[44,45]

Synthesis of the compounds

3-methoxy-4-dimethylamino-benzaldehyde (1a)

In a Schlenk flask, dimethylamine (2.83 mL, 55.96 mmol) was added stepwise (~ 2 mL per hour) to a stirred solution of 4-fluoro-3-methoxybenzaldehyde (1.73 g, 11.19 mmol) and K_2CO_3 (7.73 g, 55.96 mmol) in DMSO (18 mL) and water (6 mL). The mixture was stirred at 100°C for 5h30. The crude product was extracted with Et_2O and evaporated under vacuum. Then, it was dissolved in CH_2Cl_2 and was washed with water (3×), dried over $MgSO_4$ and evaporated under vacuum. The product was purified by silica gel chromatography (from 70/30 to 55/45 Petroleum Ether/AcOEt) to afford a yellow oil (1.96 g, 97%). ^{1}H NMR (200 MHz, $CDCl_3$) δ (ppm): 9.81 (s, 1 H), 7.34-7.44 (m, 2 H), 6.90 (d, *J*=7.9 Hz, 1 H), 3.92 (s, 3 H), 2.94 (s, 6 H). ^{13}C NMR (50 MHz, $CDCl_3$) δ (ppm): 190.35, 151.13, 147.87, 129.35, 126.37, 116.00, 108.90, 55.18, 42.20.

3-methoxy-4-diethylamino-benzaldehyde (1b)

In a Schlenk flask, diethylamine (6.82 mL, 65.88mmol) was added stepwise (~ 2 mL per hour) to a stirred solution of 4-fluoro-3-methoxybenzaldehyde (2.03 g, 13.18 mmol) and K_2CO_3 (9.11 g, 65.88 mmol) in DMSO (20 mL) and water (6 mL). The mixture was stirred at 100°C for 12h (overnight). The crude product was extracted with Et_2O and evaporated under vacuum. Then it was dissolved in CH_2Cl_2 and was washed with water (3×), dried over $MgSO_4$ and evaporated under vacuum. The product was purified by silica gel chromatography (from 70/30 to 60/40 Petroleum Ether/AcOEt) to afford a yellow oil (1.71 g, 63%). ^{1}H NMR (200 MHz, $CDCl_3$) δ (ppm): 9.77 (s, 1 H), 7.30-7.41 (m, 2H), 6.87 (d, *J*=8.8 Hz, 1 H), 3.89 (s, 3 H), 3.33(q, *J*=7.0 Hz, 4 H), 1.12 (t, *J*=7.0 Hz, 6 H). ^{13}C NMR (50 MHz, $CDCl_3$) δ (ppm): 190.58, 151.61, 146.08, 128.88, 126.56, 117.24, 109.49, 55.53, 45.65, 12.59.

Synthesis of the monostyryl BODIPY 4a

To a solution of 1,3,5,7-tetramethyl-8-(4-iodophenyl)-BODIPY[46] (0.32 g, 0.71 mmol) in toluene (50 mL) were added 3-chloro-4-hydroxy-benzaldehyde **2**[47] (0.11 g, 0.71 mmol), piperidine (70.6 µL) and p-toluenesulfonic acid (catalytic amount). The resulting mixture was stirred at reflux for 12h (overnight) using a Dean-Stark apparatus. The solution was extracted with CH_2Cl_2, washed with saturated NaCl solution (1×) and water (2×). Organics layers were dried over Na_2SO_4 and evaporated under vacuum. The product was purified by silica gel chromatography (from 99.5/0.5 to 95/5 CH_2Cl_2/MeOH) to afford starting compound BODIPY (0.26 mg), mono-styryl compound (purple) (0.052 mg, 12 %) and bis-styryl (blue) compound (0.022 mg, 4 %). ^{1}H NMR (500 MHz, CDCl3) δ (ppm): 7.86 (d, *J*=8.2 Hz, 2 H), 7.57 (d, *J*=2.1 Hz, 1 H), 7.51 (d, *J*=16.2 Hz, 1 H), 7.41 (dd, *J*=8.5, 1.8 Hz, 1 H), 7.10 (d, *J*=16.7 Hz, 1 H), 7.07 (d, *J*=8.2 Hz, 2 H), 7.02 (d, *J*=8.2 Hz, 1 H), 6.57 (s, 1 H), 6.03 (s, 1 H), 5.68 (s, 1 H), 2.60 (s, 3 H), 1.47 (s, 3 H), 1.44 (s, 3 H). ^{13}C NMR (126 MHz, $CDCl_3$) δ (ppm): 155.99, 152.65, 151.88, 142.77, 142.15, 138.75, 138.33, 134.58, 134.46, 132.46, 131.64, 130.50, 130.15, 127.88, 127.70, 121.66, 120.50, 118.15, 117.61, 116.51, 94.79, 14.90, 14.78, 14.71. ESI-HRMS, *m/z* calcd for $C_{26}H_{21}BClF_2IN_2O$: 589.0526 $[M+H]^+$; found: 589.0504 $[M+H]^+$.

General procedure A, synthesis of the 3,5-distyryl BODIPYs 4c and 4d

To a solution of 1,3,5,7-tetramethyl-8-(4-iodophenyl)-BODIPY (1 mmol, 1 eq.) in toluene (50 mL) were added the **aldehyde** (2.5 mmol, 2.5 eq.), piperidine (1 mL) and p-toluenesulfonic acid (catalytic amount). The resulting mixture was stirred at reflux for 12h using a Dean-Stark apparatus. The solution was extracted with CH_2Cl_2, washed with saturated NaCl solution (1×) and water (2×). Organics layers were dried over Na_2SO_4 and evaporated under vacuum. The product was purified by silica gel chromatography.

4c. 1,3,5,7-tetramethyl-8-(4-iodophenyl)-BODIPY (0.578 g, 1.29 mmol), aldehyde **1b** (0.666 g, 3.21 mmol). Chromatography (from 95/5 to 60/40 Petroleum Ether/AcOEt, 0.5% of Et_3N) to afford mono-styryl (blue) compound (0.167 mg, 20%) and bis-styryl (green) compound (0.364 g, 34%). ^{1}H NMR (300 MHz, $CDCl_3$) δ (ppm): 7.85 (d, *J*=8.1 Hz, 2 H), 7.59 (d, *J*=16.2 Hz, 2 H), 7.21 (d, *J*=17.1 Hz, 2 H), 7.16 (d, *J*=8.4 Hz, 2 H), 7.10 (s, 2 H), 7.10 (d, *J*=8.0 Hz, 2 H), 6.90 (d, *J*=8.4 Hz, 2 H), 6.62 (s, 2 H), 3.95 (s, 6 H), 3.25 (q, *J*=7.0 Hz, 8 H), 1.48 (s, 6 H), 1.08 (t, *J*=7.0 Hz, 12 H). ^{13}C NMR (101 MHz, $CDCl_3$) δ (ppm): 152.94, 152.90, 141.17, 140.86, 138.18, 136.60, 135.71, 134.99, 132.91, 130.63, 130.42, 121.22, 120.29, 117.79, 116.91, 109.95, 94.61, 55.53, 45.87, 14.92, 12.20. ESI-HRMS, *m/z* calcd for $C_{43}H_{49}BF_2IN_4O_2$: 829.2963 $[M+H]^+$. found: 829.3017 $[M+H]^+$.

4d. 1,3,5,7-tetramethyl-8-(4-iodophenyl)-BODIPY (0.495 mg, 1.10 mmol) aldehyde **1a** (0.493 mg, 2.75 mmol). Chromatography (from 80/20 to 60/40 Petroleum Ether/AcOEt) to afford mono-styryl (blue) compound (21.1 mg) and bis-styryl (green) compound (802.8 mg, 94%). ^{1}H NMR (300 MHz, $CDCl_3$) δ (ppm): 7.85 (d, *J*=8.2 Hz, 2 H), 7.59 (d, *J*=16.2 Hz, 2 H), 7.21 (d, *J*=16.9 Hz, 2 H), 7.16 (d, *J*=8.2 Hz, 2 H), 7.11 (s, 2 H), 7.09 (d, *J*=6.8 Hz, 2 H), 6.90 (d, *J*=8.2 Hz, 2 H), 6.63 (s, 2 H), 3.98 (s, 6 H), 2.87 (s, 12 H), 1.48 (s, 6 H). ^{13}C NMR (75 MHz, $CDCl_3$) δ (ppm): 152.92, 152.06, 143.74, 141.26, 138.20, 136.53, 135.94, 134.97, 132.96, 130.62, 121.64, 117.84, 117.74, 117.09, 109.56, 94.62, 55.48, 43.05, 14.90. ESI-HRMS, *m/z* calcd for $C_{39}H_{40}BF_2IN_4O_2$: 772.2258 $[M]^+$; found: 772.2279 $[M]^+$.

General procedure B: synthesis of boron disubstituted BODIPY dyes 5a-e

In a Schlenk flask, ethylmagnesiumbromide 1 M solution in THF (4.5 eq.) was added to a stirred solution of 3-dimethylamino-1-propyne (5 eq.) in

Accepted Manuscript

This article is protected by copyright. All rights reserved.

anhydrous THF (6 mL). The mixture was stirred at 60°C for 12h (overnight) under argon. The resulting anion was then transferred with a canula to a solution of difluoro-**BODIPY** (1equiv) in anhydrous THF (6 mL). The solution was stirred at 60°C for 15 min under argon. Water was added, and the solution was extracted with CH_2Cl_2 which contains MeOH. The organic phase was washed with water (3×), dried over $MgSO_4$ and evaporated under vacuum. The product was purified by silica gel chromatography

5a. Ethylmagnesiumbromide 1 M solution in THF (0.59 mL, 0.59 mmol), 3-dimethylamino-1-propyne (73 µL, 0.68 mmol), BODIPY **4a** (74 mg, 0.13 mmol. Chromatography (from 98/2 to 94/6 CH_2Cl_2/MeOH) to afford a purple compound (44.1 mg, 49%). ^{1}H NMR (300 MHz, $CDCl_3$) δ (ppm): 8.12 (d, *J*=16.2 Hz, 1 H), 7.85 (d, *J*=8.1 Hz, 2 H), 7.55 (s, 1 H), 7.34 (d, *J*=8.6 Hz, 1 H), 7.10 (d, *J*=8.3 Hz, 2 H), 7.02 (d, *J*=16.4 Hz, 1 H), 6.90 (d, *J*=8.5 Hz, 1 H), 6.60 (s, 1 H), 6.08 (s, 1 H), 3.37 (s, 2 H), 3.36 (s, 2 H), 2.78 (s, 3 H), 2.34 (s, 12 H), 1.47 (s, 3 H), 1.44 (s, 3 H). ^{13}C NMR (75 MHz, $CDCl_3$) δ (ppm): 155.65, 153.66, 151.60, 141.10, 140.39, 138.84, 138.25, 134.98, 132.53, 130.57, 130.33, 130.01, 127.90, 127.20, 122.01, 121.45, 117.90, 117.39, 94.64, 88.88, 48.55, 43.44, 16.42, 15.12, 14.95. ESI-HRMS, *m/z* calcd for $C_{36}H_{38}BClIN_4O$: 715.1873 $[M+H]^+$; found: 715.1798 $[M+H]^+$.

5b. Ethylmagnesiumbromide 1 M in THF (1 mL, 1.0 mmol), 3-dimethylamino-1-propyne (125.7 µL, 1.17 mmol), BODIPY **4b**[26] (0.2 g, 0.29 mmol). Chromatography (from 96/4 to 92/8 CH_2Cl_2/MeOH) to afford a green compound (0.21 g, 88%) ^{1}H NMR (300 MHz, $CDCl_3$) δ (ppm): 8.09 (2d, *J*=16.0 Hz, 2 H), 7.84 (d, 7.9 Hz, 2 H), 7.51 (2d, *J*=8.3 Hz, *J*=8.2 Hz, 4 H), 7.06-7.21 (m, 4 H), 6.80 (d, *J*=8.3 Hz, 2 H), 6.69 (d, *J*=8.9 Hz, 2 H), 6.65 (s, 1 H), 6.61 (s, 1 H), 3.35 (s, 4 H), 3.04 (s, 6 H), 2.29 (s, 12 H), 1.47 (2s, 6 H). ^{13}C NMR (75 MHz, $CDCl_3$) δ (ppm): 158.81, 153.02, 151.26, 150.90, 140.13, 139.11, 138.06, 135.66, 135.41, 133.83, 131.32, 130.85, 128.94, 128.88, 128.57, 125.02, 118.53, 118.14, 117.63, 116.35, 112.08, 94.44, 48.50, 43.33, 40.23, 15.19, 15.09. ESI-HRMS, *m/z* calcd for $C_{45}H_{48}BIN_5O$: 812.2999 $[M+H]^+$; found: 812.2970 $[M+H]^+$.

5c. Ethylmagnesiumbromide 1 M in THF (0.85 mL, 0.86 mmol), 3-dimethylamino-1-propyne (0.105 mL, 0.98 mmol), BODIPY **4c** (0.200 g, 0.24 mmol) Chromatography (from 98/2/0 to 94/6/1 CH_2Cl_2/MeOH/Et_3N) to afford a green compound (0.192 mg, 83%). ^{1}H NMR (300 MHz, $CDCl_3$) δ (ppm): 8.22 (d, *J*=16.3 Hz, 2 H), 7.83 (d, *J*=8.2 Hz, 2 H), 7.19 (d, *J*=8.2 Hz, 2 H), 7.11-7.16 (m, 4 H), 7.10 (s, 2 H), 6.90 (d, *J*=8.2 Hz, 2 H), 6.63 (s, 2 H), 3.93 (s, 6 H), 3.24 (q, *J*=7.1 Hz, 8 H), 3.20 (s, 4 H), 2.16 (s, 12 H), 1.45 (s, 6 H), 1.08 (t, *J*=7.1 Hz, 12 H). ^{13}C NMR (75 MHz, $CDCl_3$) δ (ppm): 152.96, 151.98, 140.35, 139.53, 138.01, 136.14, 135.41, 134.19, 131.24, 131.15, 130.75, 120.56, 120.41, 119.46, 118.00, 110.14, 94.38, 89.99, 55.29, 48.85, 45.88, 43.92, 15.09, 12.14. ESI-HRMS, *m/z* calcd for $C_{53}H_{65}BIN_6O_2$: 955.4310 $[M+H]^+$; found: 955.4445 $[M+H]^+$.

5d. Ethylmagnesiumbromide 1 M in THF (0.90 mL, 0.91 mmol), 3-dimethylamino-1-propyne (0.11 mL, 1.04 mmol) BODIPY **4d** (0.20 g, 0.26 mmol) Chromatography (from 98/2 to 94/6 CH_2Cl_2/MeOH) to afford a green compound (0.218 g, 95%). ^{1}H NMR (200 MHz, $CDCl_3$) δ (ppm): 8.22 (d, *J*=16.3 Hz, 2 H), 7.83 (d, *J*=8.0 Hz, 2 H), 7.06-7.25 (m, 8 H), 6.90 (d, *J*=8.1 Hz, 2 H), 6.64 (s, 2 H), 3.97 (s, 6 H), 3.20 (s, 4 H), 2.86 (s, 12 H), 2.17 (s, 12 H), 1.45 (s, 6 H). ^{13}C NMR (75 MHz, $CDCl_3$) δ (ppm): 152.00, 143.31, 139.60, 138.05, 136.30, 135.41, 134.11, 131.28, 131.25, 130.75, 121.07, 119.50, 118.03, 117.71, 109.63, 94.40, 90.03, 55.21, 48.88, 43.97, 43.07, 15.09. ESI-HRMS, *m/z* calcd for $C_{49}H_{57}BIN_6O_2$: 899.3684 $[M+H]^+$; found: 899.3663 $[M+H]^+$.

5e. Ethylmagnesiumbromide 1 M in THF (0.67 mL, 0.68 mmol), 3-dimethylamino-1-propyne (0.10 mL, 0.90 mmol), BODIPY **4e** (0.20 g, 0.28 mmol). Chromatography (from 98/2 to 92/8 CH_2Cl_2/MeOH) to afford a green compound (0.234 g, 99%). ^{1}H NMR (300 MHz, $CDCl_3$) δ (ppm): 8.14 (d, *J*=16.2 Hz, 2 H), 7.80 (d, *J*=8.2 Hz, 2 H), 7.55 (d, *J*=8.6 Hz, 4 H), 7.11 (d, *J*=16.1 Hz, 2 H), 7.09 (d, *J*=8.2 Hz, 2 H), 6.71 (d, *J*=8.6 Hz, 4 H), 6.61 (s, 2 H), 3.25 (s, 4 H), 3.02 (s, 12 H), 2.24 (s, 12 H), 1.43 (s, 6 H). ^{13}C NMR (75 MHz, $CDCl_3$) δ (ppm): 152.05, 150.53, 138.94, 137.82, 135.56, 134.89, 134.36, 130.89, 130.86, 128.71, 125.44, 117.62, 117.04, 111.97, 94.17, 89.38, 48.74, 43.75, 40.15, 14.98. ESI-HRMS, *m/z* calcd for $C_{47}H_{53}BIN_6$: 839.3472 $[M+H]^+$; found: 839.3497 $[M+H]^+$.

General procedure C: carboxylation of the styryl BODIPY derivatives.

To a solution of 8-(4-iodophenyl)-BODIPY derivative (1 eq., 0.2 mmol) in absolute ethanol (10 mL) and triethylamine (10 mL) was added $Pd(PPh_3)_2Cl_2$ (5%mol, 0.01 mmol). The resulting mixture was stirred at 70°C for 12h (night) under a slow bubbling CO gas flux. The crude product was washed with water (3×) and extracted with CH_2Cl_2. Organics layers were dried over Na_2SO_4 and evaporated under vacuum. The product was purified by silica gel chromatography.

6a. Compound **5a** (39.6 mg, 0.05 mmol), $Pd(PPh_3)_2Cl_2$ (2.3 mg, 0.003 mmol). Chromatography (from 96/3/1 to 94/5/1 CH_2Cl_2/MeOH/Et_3N) to afford a purple compound (35.4 mg, 97%). ^{1}H NMR (200 MHz, $CDCl_3$) δ ppm: 8.19 (d, *J*=8.0 Hz, 2 H), 8.04 (d, *J*=15.8 Hz, 1 H), 7.40-7.60 (m, 4 H), 7.18 (d, *J*=8.5 Hz, 1 H), 7.05 (d, *J*=16.2 Hz, 1 H), 6.60 (s, 1 H), 6.07 (s, 1 H), 4.44 (q, *J*=7.1 Hz, 2 H), 3.53 (s, 4 H), 2.76 (s, 3 H), 2.45 (s, 12 H), 1.31-1.55 (m, 9 H). ESI-HRMS, *m/z* calcd for $C_{39}H_{43}BClN_4O_3$: 661.3118 $[M+H]^+$; found: 661.3138 $[M+H]^+$.

6b. Compound **5b** (146.0 mg, 0.18 mmol) $Pd(PPh_3)_2Cl_2$ (7.6 mg, 0.01 mmol). Chromatography (from 100/0 to 90/10 CH_2Cl_2/MeOH) to afford a green compound (87.4 mg, 64%). ^{1}H NMR (300 MHz, $CDCl_3$) δ (ppm): 8.18 (d, *J*=7.9 Hz, 2 H), 8.08 (2d, *J*=16.9 Hz, *J*=16.5 Hz, 2 H), 7.49 (2d, *J*=9.6 Hz, *J*=8.6 Hz, 6 H), 7.16 (d, *J*=16.2 Hz, 1 H), 7.11 (d, *J*=16.2 Hz, 1 H), 6.84 (d, *J*=8.3 Hz, 2 H), 6.69 (d, *J*=8.9 Hz, 2 H), 6.65 (s, 1 H), 6.61 (s, 1 H), 4.43 (q, *J*=7.1 Hz, 2 H), 3.37 (s, 2 H), 3.35 (s, 2 H), 3.04 (s, 6 H), 2.31 (s, 12 H), 1.44 (t, *J*=7.2 Hz, 6 H), 1.41 (s, 3 H).^{13}C NMR (75 MHz, $CDCl_3$) δ (ppm): 166.15, 159.00, 153.15, 151.24, 150.96, 140.58, 140.18, 139.08, 135.90, 135.78, 133.98, 131.14, 130.85, 130.57, 130.06, 129.19, 128.95, 128.89, 128.45, 124.95, 118.40, 118.20, 117.66, 116.42, 116.31, 112.13, 88.04, 61.31, 48.50, 43.25, 40.22, 15.04, 14.92, 14.30. ESI-HRMS, *m/z* for calcd $C_{48}H_{53}BN_5O_3$: 758.4244 $[M+H]^+$; found: 758.4251 $[M+H]^+$.

6c. General procedure C: **5c** (52.7 mg, 0.06 mmol), $Pd(PPh_3)_2Cl_2$ (2.3 mg, 0.003 mmol). Chromatography (from 99/0.5/0.5 to 97/2.5/0.5 CH_2Cl_2/MeOH/Et_3N) to afford a green compound (48.9 mg, 98%). ^{1}H NMR (200 MHz, CDCl3) δ (ppm): 8.16 (2d, *J*=16.8 Hz, *J*=7.4 Hz, 4 H), 7.48 (d, *J*=8.0 Hz, 2 H), 7.14-7.25 (m, 4 H), 7.09 (s, 2 H), 6.91 (d, *J*=8.4 Hz, 2 H), 6.64 (s, 2 H), 4.44 (q, *J*=7.0 Hz, 2 H), 3.93 (s, 6 H), 3.15-3.35 (m, 12 H), 2.23 (s, 12 H), 1.35-1.52 (m, 9 H), 1.08 (t, *J*=6.9 Hz, 12 H). ^{13}C NMR (50 MHz, CDCl3) δ (ppm): 166.03, 152.72, 151.96, 140.29, 140.10, 135.28, 132.19, 131.99, 131.94, 131.89, 131.08, 130.17, 129.01, 128.60, 128.35, 120.27, 119.73, 118.27, 111.57, 61.40, 55.70, 48.12, 45.84, 42.28, 29.66, 15.03, 14.32, 12.40. ESI-HRMS, *m/z* calcd for $C_{56}H_{70}BN_6O_4$: 901.5555 $[M+H]^+$; found: 901.5587 $[M+H]^+$.

6d. Compound **5d** (81.3 mg, 0.09 mmol), $Pd(PPh_3)_2Cl_2$ (3.8 mg, 0.005 mmol). Chromatography (from 98/2 to 94/6 CH_2Cl_2/MeOH/Et_3N) to afford a green compound (72.1 mg, 94%). ^{1}H NMR (400 MHz, $CDCl_3$) δ (ppm): 8.18 (2d, *J*=16.4 Hz, *J*=8.1 Hz, 4 H), 7.48 (d, *J*=8.2 Hz, 2 H), 7.20 (d, *J*=8.2 Hz, 2 H), 7.14 (d, *J*=16.2 Hz, 2 H), 7.12 (s, 2 H), 6.90 (d, *J*=8.2 Hz, 2 H), 6.64 (s, 2 H), 4.44 (q, *J*=7.1 Hz, 2 H), 3.96 (s, 6 H), 3.27 (s, 4 H),

Accepted Manuscript

This article is protected by copyright. All rights reserved.

2.87 (s, 12 H), 2.23 (s, 12 H), 1.45 (t, *J*=7.2 Hz, 3 H), 1.42 (s, 6 H). ^{13}C NMR (101 MHz, $CDCl_3$) δ (ppm): 166.13, 152.07, 152.03, 143.52, 140.53, 139.82, 136.65, 134.45, 131.12, 131.02, 130.91, 130.11, 129.09, 120.84, 119.21, 118.17, 117.81, 109.99, 61.34, 55.33, 48.76, 45.85, 43.63, 43.08, 15.02, 14.32. ESI-HRMS, *m/z* calcd for $C_{52}H_{62}BN_6O_4$: 845.4929 $[M+H]^+$; found: 845.4858 $[M+H]^+$.

6e. Compound **5e** (197 mg, 0.24 mmol), $Pd(PPh_3)_2Cl_2$ (9.9 mg, 0.01 mmol). Chromatography (from 100/0 to 90/10 CH_2Cl_2/MeOH) to afford a green compound (166 mg, 90%). ^{1}H NMR (200 MHz, $CDCl_3$) δ (ppm): 8.14 (2d, *J*=8.0 Hz, *J*=16.2 Hz, 4 H), 7.53 (d, *J*=8.6 Hz, 4 H), 7.44 (d, *J*=8.0 Hz, 2 H), 7.10 (d, *J*=16.2 Hz, 2 H), 6.70 (d, *J*=8.8 Hz, 4 H), 6.60 (s, 2 H), 4.41 (q, *J*=7.2 Hz, 2 H), 3.27 (s, 4 H), 3.02 (s, 12 H), 2.25 (s, 12 H), 1.43 (t, *J*=7.2 Hz, 3 H), 1.39 (s, 6 H). ^{13}C NMR (50 MHz, $CDCl_3$) δ (ppm): 166.02, 152.04, 150.54, 140.73, 138.94, 135.07, 134.51, 130.63, 130.51, 129.81, 129.11, 128.66, 125.21, 117.60, 116.77, 111.92, 88.78, 61.10, 48.57, 43.49, 40.08, 14.79, 14.15. ESI-HRMS, m/z calcd for $C_{50}H_{58}BN_6O_2$: 785.4717 $[M+H]^+$; found: 785.4799 $[M+H]^+$.

General procedure D: sultonation of tertiary amine.

In a Schlenk flask, 1,3-propane sultone (0.25 mmol, 5 eq.) was added to a solution of bis-(dimethylamino-propyne)-BODIPY (0.05 mmol, 1eq.) in DMF distilled (2 mL). The mixture was stirred at room temperature for 2 days (week end) under argon. The product was obtained by precipitation thanks to addition of ethyl acetate to the solution. The precipitate was centrifuged and washed with ethyl acetate (3×) and pentane (1×). The precipitate can be recrystallized in EtOH/AcOEt and washed with pentane to afford the desired compound

7a. 1,3-propane sultone (22.9 µL, 0.26 mmol), **6a** (34.5 mg, 0.05 mmol). Purple compound (38.8 mg, 82%). ^{1}H NMR (300 MHz, CD_3OD) δ (ppm): 8.23 (d, *J*=7.9 Hz, 2 H), 7.88 (d, *J*=16.2 Hz, 1 H), 7.52-7.59 (m, 4 H), 7.38 (d, *J*=16.4 Hz, 1 H), 7.10 (d, *J*=8.9 Hz, 1 H), 6.87 (s, 1 H), 6.23 (s, 1 H), 4.43 (q, *J*=7.3, 7.1 Hz, 2 H), 4.31 (s, 2 H), 4.30 (s, 2 H), 3.42-3.57 (m, 4 H), 3.05 (s, 12 H), 2.68-2.78 (m, 7 H), 2.07-2.21 (m, 4 H), 1.37-1.50 (m, 9 H). ^{13}C NMR (75 MHz, CD_3OD) δ (ppm): 181.66, 167.47, 157.39, 156.22, 153.36, 143.75, 143.14, 141.33, 141.12, 136.22, 132.79, 131.72, 131.67, 131.22, 130.67, 130.56, 130.32, 127.83, 123.64, 122.77, 119.82, 118.98, 118.71, 64.11, 62.67, 56.51, 51.12, 51.07, 35.53, 23.13, 20.16, 16.89, 15.27, 15.12, 14.74, 9.34. ESI-HRMS, *m/z* calcd for $C_{45}H_{55}BClN_4O_9S_2$: 905.3194 $[M+H]^+$; found: 905.3145 $[M+H]^+$.

7b. 1,3-propane sultone (56.5 µL, 0.64 mmol), **6b** (97.6 mg, 0.13 mmol). Green compound (54.2 mg, 42%). ^{1}H NMR (200 MHz, CD_3OD) δ (ppm): 8.23 (d, *J*=8.1 Hz, 2 H), 7.86 (2d, *J*=16.1 Hz, 2 H), 7.50-7.66 (m, 6 H), 7.37 (2d, *J*=16.0 Hz, *J*=16.2 Hz, 2 H), 6.78-6.98 (m, 6 H), 4.44 (q, *J*=7.1 Hz, 2 H), 4.28 (s, 4 H), 3.37-3.51 (m, 4 H), 3.07 (s, 6 H), 2.97 (s, 12 H), 2.69 (t, *J*=6.8 Hz, 4 H), 2.02-2.18 (m, 4 H), 1.36-1.53 (m, 9 H). ^{13}C NMR (101 MHz, CD_3OD) δ (ppm): 173.28, 172.67, 154.78, 152.61, 142.74, 141.60, 141.41, 137.58, 136.84, 132.57, 132.49, 131.86, 131.48, 130.78, 130.53, 130.32, 130.05, 129.34, 126.43 125.60, 119.80, 119.16, 117.79, 115.48, 113.92, 111.65, 63.94, 62.69, 61.73, 56.70, 51.03, 40.51, 20.11, 15.31, 15.18, 14.74, 14.58. ESI-HRMS, *m/z* calcd for $C_{54}H_{64}BN_5NaO_9S_2$: 1024.4140 $[M+Na]^+$; found: 1024.4109 $[M+Na]^+$.

7c. 1,3-propane sultone (19.4 µL, 0.22 mmol), **6c** (39.9 mg, 0.04 mmol). Brown compound (25.5 mg, 50%). ^{1}H NMR (200 MHz, CD_3OD) δ (ppm): 8.24 (d, *J*=8.0 Hz, 2 H), 7.96 (d, *J*=16.2 Hz, 2 H), 7.59 (d, *J*=8.2 Hz, 2 H), 7.39-7.53 (m, 4 H), 7.08-7.26 (m, 4 H), 6.91 (s, 2 H), 4.44 (q, *J*=7.0 Hz, 2 H), 4.29 (s, 4 H), 3.94 (s, 6 H), 3.35-3.48 (m, 4 H), 2.96 (s, 12 H), 2.63 (t, *J*=6.8 Hz, 4 H), 1.97-2.14 (m, 4 H), 1.49 (s, 6 H), 1.44 (t, *J*=7.0 Hz, 3 H), 1.10 (t, *J*=7.0 Hz, 12 H). ESI-HRMS, *m/z* calcd for $C_{62}H_{82}BN_6O_{10}S_2$: 1145.5632 $[M+H]^+$; found: 1145.5591 $[M+H]^+$.

7d. 1,3-propane sultone (20.8 µL, 0.24 mmol), **6d** (40.1 mg, 0.05 mmol). Brown compound (32.4 mg, 63%). ^{1}H NMR (200 MHz, CD_3OD) δ (ppm): 8.24 (d, *J*=8.2 Hz, 2 H), 7.96 (d, *J*=16.1 Hz, 2 H), 7.58 (d, *J*=8.3 Hz, 2 H), 7.38-7.52 (m, 4 H), 7.19 (d, *J*=8.5 Hz, 2 H), 7.12 (s, 2 H), 6.90 (s, 2 H), 4.44 (q, *J*=7.1 Hz, 2 H), 4.29 (s, 4 H), 3.95 (s, 6 H), 3.35-3.48 (m, 4 H), 2.97 (s, 12 H), 2.87 (s, 12 H), 2.53-2.67 (m, 4 H), 1.95-2.16 (m, 4 H), 1.49 (s, 6 H), 1.44 (t, *J*=7.1 Hz, 3 H). ^{13}C NMR (100 MHz, CD_3OD) δ (ppm): 167.53, 153.70, 153.57, 145.18, 142.63, 141.36, 138.70, 137.88, 132.75, 132.52, 132.11, 131.59, 130.70, 120.54, 120.08, 119.95, 118.59, 113.89, 84.78, 63.90, 62.68, 56.63, 56.44, 50.97, 43.58, 23.54, 20.13, 15.32, 14.76, 14.51. ESI-HRMS, *m/z* calcd for $C_{58}H_{74}BN_6O_{10}S_2$: 1089.5005 $[M+H]^+$; found: 1089.5031 $[M+H]^+$.

7e. 1,3-propane sultone (62 µL, 0.71 mmol), **6e** (111.1 mg, 0.14 mmol). Brown compound (79.8 mg, 55%). ^{1}H NMR (300 MHz, CD_3OD) δ (ppm): 8.21 (d, *J*=8.1 Hz, 2 H), 7.84 (d, *J*=16.0 Hz, 2 H), 7.58 (d, *J*=8.7 Hz, 4 H), 7.53 (d, *J*=8.1 Hz, 2 H), 7.35 (d, *J*=16.0 Hz, 2 H), 6.89 (d, *J*=8.7 Hz, 4 H), 6.81 (s, 2 H), 4.43 (q, *J*=7.1 Hz, 2 H), 4.27 (s, 4 H), 3.40-3.50 (m, 4 H), 3.06 (s, 12 H), 2.97 (s, 12 H), 2.68 (t, *J*=6.7 Hz, 4 H), 2.02-2.16 (m, 4 H), 1.37-1.49 (m, 9 H). ^{13}C NMR (75 MHz, CD_3OD) δ (ppm): 167.60, 153.71, 153.26, 141.76, 138.07, 132.55, 132.13, 131.47, 130.88, 130.36, 125.85, 119.37, 115.87, 113.95, 63.91, 62.66, 56.75, 51.02, 40.55, 20.14, 15.29, 14.76. ESI-HRMS, *m/z* calcd for $C_{56}H_{70}BN_6O_8S_2$: 1029.4794 $[M+H]^+$; found: 1029.4772 $[M+H]^+$.

Acknowledgements

The authors wish to thank the International Center for Frontier Research in Chemistry (ic-FRC) in Strasbourg (Innovation 2012, project entitled "*Innovative Environmental Sensitive Dyes (ESDyes) for monitoring pH and redox changes found in human pathogen malarial parasites"* for creating a proper framework for this scientific collaboration. G.U. and M.E. thanks the Centre National de la Recherche Scientifique and the University of Strasbourg (UMR 7042 and UMR 7515) in France for financial support.

Keywords: BODIPY • Titration • pH probes • fluorescence •

Accepted Manuscript

This article is protected by copyright. All rights reserved.

[1] J. Han, K. Burgess, *Chem. Rev.* **2010**, *110*, 2709-2728.
[2] G. Grynkiewicz, M. Poenie, R. Y. Tsien, *J. Biol. Chem*. **1985**, *260*, 3440-3450.
[3] R.Weissleder, *Nature Biotech*. **2001**, *19*, 316-317; R. Weissleder, V. Ntziachristos *Nature Med*. **2003**, *9*, 123-128
[4] T. J. Rink, R.Y. Tsien, T. J. Pozzan, *Cell. Biol*, **1982**, *95*, 189-196.
[5] J. E. Whitaker, R. P. Haughland, F. G. Prendergast, *Anal. Biochem*. **1991**, *194*, 330-344; M. Taggart, C. Austin, S. Wray, *J. Physiol*. **1994**, *475*, 285-292.
[6] O. Seksek, N. Henry-Toulme, Sureau, F.; Bolard, *J. Anal. Biochem.* **1991**, *193*, 49-54.
[7] Asanuma, D.; Takaoka, Y.; S. Namiki, K. Takikawa, M. Kamiya, T. Nagano, Y. Urano, K. Hirose, *Angew. Chem., Int. Ed.* **2014**, *53*, 6085-6089.
[8] M. Ipuy, C. Billon, G. Micouin, J. Samarut, C. Andraud, Y. Bretonnière, *Org. Biomol. Chem*. **2014**, *12*, 3641-3648.
[9] Q. Wang, L. Zhou, L. Qiu, D. Lu, Y. Wu, X.-B. Zhang, *Analyst* **2015**, *140*, 5563-5569.
[10] S. Charier, O. Ruel, J.-B. Baudin, D. Alcor, J.-F. Allemand, A. Meglio, L. Jullien, *Angew. Chem., Int. Ed*. **2004**, *43*, 4785-4788.
[11] H. J. Kim, C. H. Heo, H. M. Kim. *J. Am. Chem. Soc.* **2013**, *135*, 17969-17977.
[12] A. Loudet, K. Burgess, *Chem. Rev.* **2007**, *107*, 4891-4932.
[13] G. Ulrich, A. Harriman, R. Ziessel *Angew. Chem., Int. Ed*. **2008**, *47*, 1202-1219.
[14] N. Boens, V. Leen, W. Dehaen, *Chem. Soc. Rev*. **2012**, *41*, 1130-1172.
[15] W. Qin, M. Baruah, W. M. De Borggraeve, N. J. Boens *Photochem. Photobiol. A: Chem*., **2006**, *183*, 190-197. F. Xue, P. Wei, X. Ge, Y. Zhong, C. Cao, D. Yu, T. Yi, Dyes Pigments **2018**, *156*, 285–290. S. Radunz, H. R. Tschiche, D. Moldenhauer, U. Resch-Genger, *Sensors and Actuators B: Chemical* **2017**, *251*, 490–494. [1]R. Gotor, P. Ashokkumar, M. Hecht, K. Keil, K. Rurack, *Anal. Chem*. **2017**, *89*, 8437–8444.
[16] Y. Ni, J. Wu, *Org. Biomol. Chem*. **2014**, *12*, 3774-3791; H. Xiong, P. Kos, Y. Yan, K. Zhou, J. B. Miller, S. Elkassih, D. J. Siegwart, *Bioconjugate Chem*. **2016**, *27*, 1737–1744; H. Xiong, H. Zuo, Y. Yan, G. Occhialini, K. Zhou, Y. Wan, D. J. Siegwart, *Advanced Materials* **2017**, *29*, 1700131.
[17] T. Jokic, S. M. Borisov, R. Saf, D. A. Nielsen, M. Kühl, I. Klimant, *Anal. Chem.* **2012**, *84*, 6723-6730; J. Tian, J. Zhou, Z. Shen, L. Ding, J.-S. Yu, H. Ju, *Chem. Sci.* **2015**, 6, 5969–5977. M. Strobl, T. Rappitsch, S. M. Borisov, T. Mayr, I. Klimant *Analyst*, **2015**, *140*, 7150-7153
[18] Y. Urano, D. Asanuma, Y. Hama, Y. Koyama, T. Barrett, M. Kamiya, T. Nagano, T. Watanabe, A. Hasegawa, P. L. Choyke, H. Kobayashi, *Nat. Med.* 2009, 15, 104-109.
[19] S. Hoogendoorn, A. E. M. Blom, L. I. Willems, G. A. van der Marel, H. S. Overkleeft, *Org. Lett.* **2011**, *13*, 5656-5659.
[20] S.-L. Niu, G. Ulrich, R. Ziessel, A. Kiss, P.-Y. Renard, A. Romieu *Org. Lett*. **2009**, *11*, 2049-2052.
[21] Niu, S. L.; Massif, C.; Ulrich, G.; Ziessel, R.; Renard, P.-Y.; Romieu, A. *Org. Biomol. Chem.* **2010**, *9*, 66–69.
[22] E. Muro, A. Fragola, T. Pons, N. Lequeux, A. Ioannou, P. Skourides, B. Dubertret, *Small*, **2012**, *8*, 1029-1037.
[23] P. Didier, G. Ulrich, Y. Mély, R. Ziessel, *Org. Biomol. Chem*., **2009**, *7*, 3639-3642.
[24] S. Erbas-Cakmak, E. U. Akkaya*, Angew. Chem. Int. Ed.* **2013**, *52*, 11364–11368; O. A. Bozdemir, R. Guliyev, O. Buyukcakir, S. Selcuk, S. Kolemen, G. Gulseren, T. Nalbantoglu, H. Boyaci, Akkaya, E. U. *J. Am. Chem. Soc*. **2010**, *132*, 8029–8036; R. Guliyev, S. Ozturk, Z. Kostereli, E. U. Akkaya, *Angew. Chem. Int. Ed.* **2011**, *50*, 9826–9831.
[25] R. Ziessel, G. Ulrich, A. Harriman, M. A. H. Alamiry, B. Stewart, P. Retailleau, *Chem. Eur. J*. **2009**, *15*, 1359-1369
[26] T. Bura, P. Retailleau, G. Ulrich, R. Ziessel, *J. Org. Chem.* **2011**, *76*, 1109-1117; R. Ziessel, G. Ulrich, A. Harriman, M. A. H. Alamiry, B. Stewart, P. Retailleau, *Chem. Eur. J.,* **2009**, **15**, 1359-1369.
[27] E. Deniz, G. C. Isbasar, Ö. A. Bozdemir, L. T. Yildirim, A. Siemiarczuk, E. U. Akkaya, *Org. Lett.* **2008**, *10*, 3401–3403; G. Barin, M. D. Yilmaz, E. U. Akkaya, *Tetrahedron Lett.* **2009**, *50*, 1738–1740; O. Buyukcakir, O. A. Bozdemir, S. Kolemen, S. Erbas, E. U. Akkaya, *Org. Lett*. **2009**, *11*, 4644–4647.
[28] T. Takahashi, I. Hijikuro, H. Sugimoto, T. Kihara, Y. Shimmyo, T. Niidome,; PCT Int. Appl. (2008), WO 2008066151 A1 20080605.
[29] A. Speicher, J. Kolz, R.P. Sambanje*, Synthesis*, **2002**, 2503-2512
[30] A. Desai, R. Milburn, *J. Am. Chem. Soc.* **1969**, *91*,1958-1961.
[31] S.-L. Niu, C. Massif, G. Ulrich, P.-Y. Renard, A. Romieu, R. Ziessel, *Chem. Eur. J.* **2012**, *18*, 7229-7242
[32] G. Ulrich, A. Haefele, P. Retailleau, R. Ziessel, *J. Org. Chem.* **2012**, *77*, 5036-5048
[33] A. Filarowski, M. Kluba, K. Cieślik-Boczula, A. Koll, A. Kochel, L.;Pandey, W. M. D. Borggraeve, M. V. der Auweraer, J. Catalán, N. Boens, *Photochemical & Photobiological Sciences* **2010**, *9*, 996–1008.
[34] J. III. Olmsted, *J. Phys. Chem.* **1979**, *83*, 2581.
[35] G. Ulrich, S. Goeb, A. De Nicola, P. Retailleau, R. Ziessel, *J. Org. Chem*. **2011**, *76*, 4489–4505.
[36] www.photochemcad.com; H. Du, R.-C. A. Fuh, J. Li, L. A. Corkan, J. S. Lindsey, *Photochem. Photobiol.*, **1998**, *68*, 141-142; J. M. Dixon, M. Taniguchi, J. S. Lindsey, *Photochem. Photobiol*. **2005**, *81*, 212-213
[37] T. Bura, P. Retailleau, G. Ulrich, R.Ziessel, *J. Org. Chem*. **2011**, *76*, 1109-1117.
[38] D. D. Perrin, B. Dempsey, E. P. Serjeant, pKa Prediction for Organic Acids and Bases, Chapman and Hall, London, 1981; A. Albert, E. P. Serjeant, The Determination of Ionization Constants, Third Edition, Chapman and Hall, London, 1984; M.J. O' Neil, Ed., The Merck Index, 14th Edition, Merck & Co., Whitehouse Station, NJ, 2006.
[39] A. Reznik, L. Pokrovskaya, N. Doroshenko, *Zh. Neorg. Khim*. **1978**, *23*, 40.
[40] P. Gans, B. O'Sullivan, *Talanta* **2000**, *51*, 33-37.
[41] H. Gampp, M. Maeder, C. J. Meyer, A. D. Zuberbühler, *Talanta*. **1985**, *32*, 95.
[42] H. Gampp, M. Maeder, C. J. Meyer, A. D. Zuberbühler *Talanta*. **1985**, *32*, 251.
[43] H. Gampp, M. Maeder, C. J. Meyer, A. D. Zuberbühler *Talanta* . **1985**, *32*, 1133.
[44] D. W. Marquardt, *J. Soc. Indust. Appl. Math*. **1963**, *11*, 431-441.
[45] M. Maeder, A. D. Zuberbühler, *Anal. Chem*. **1990**, *62*, 2220-2224.
[46] L. Bonardi, G. Ulrich, R. Ziessel, *Org. Lett*. **2008**, *10*, 2183–2186.
[47] A. Speicher, J. Kolz, R. P. Sambanje, *Synthesis* **2002**, 2503–2512.

Accepted Manuscript

This article is protected by copyright. All rights reserved.